ELSEVIER

Diamond and Related Materials 7 (1998) 123–128

DIAMOND AND RELATED MATERIALS

Electrical and structural properties of AlGaN: a comparison with CVD diamond

M. Stutzmann *, O. Ambacher, H. Angerer, C.E. Nebel, E. Rohrer

Walter Schottky Institut, Technische Universität München, Am Coulombwall, D-85748 Garching, Germany

Received 23 June 1997; accepted 19 August 1997

Abstract

The present state of the AlGaN system is discussed in comparison to the known properties of CVD diamond. Growth and structural features of thin films as well as heterostructures are described. The variation of the fundamental optical gap with aluminum content provides the basis for the application of AlGaN in optical devices for the ultraviolet spectral range. The large conduction band offset between GaN and AlN together with reasonable dopability of AlGaN allow the construction of new field effect transistors with promising performance. The use of AlGaN in surface acoustic wave devices and the potentially negative electron affinity of alloys with high Al content are also briefly mentioned. © 1998 Elsevier Science S.A.

Keywords: Doping; Optoelectronic properties; Growth; Device

1. Introduction

Compared with SiC, both diamond and the group III-nitrides (InN, GaN, and AlN) are relative newcomers in the competiton for electronic applications requiring wide-bandgap materials. Whereas at present SiC is most advanced as far as technological and device issues are concerned [1], and diamond would be the material of choice for many applications because of its excellent electronic and thermal properties, the group III-nitrides currently experience a very rapid development and show a lot of promise for the future. In contrast to SiC and diamond, but similar to the group II–VI compounds, all group III-nitrides have a direct bandgap (at least in the wurtzite structure) and allow the preparation of heterostructures with largely variable band offsets within the same material system. Whether these advantages are sufficient to overcome the known problems of GaN and Co (lack of bulk crystals with sufficient size, large lattice mismatches with the by now established substrate materials sapphire and SiC, low hole mobilities and thermal conductivities) remains to be seen.

So far, most of the work published about the group III-nitrides covers GaN and its alloys with small In or Al concentrations, i.e., the materials currently used in commercial light-emitting diodes and various transistor prototypes. There exist a number of excellent reviews concerning these Ga-rich alloys, and the reader is referred to the relevant literature for more details [2–4]. The purpose of this article is to concentrate more on the structural and electronic properties of the AlGaN alloy system, in particular the Al-rich alloys with bandgaps comparable with that of diamond.

2. Preparation and structure

Device quality group III-nitrides are usually grown by metal-organic chemical vapor deposition (MOCVD) or molecular beam epitaxy (MBE) on SiC or Al_2O_3 substrates with typical growth rates of approx. 1 μm/h. Much higher growth rates can be achieved by hydride vapor phase epitaxy (HVPE), alas at the expense of the film quality. Typical growth temperatures for AlGaN alloys are in the range 850–1100 °C, depending on the growth method and the Al concentration. Because of the large lattice mismatch between AlGaN and the common substrates, the use of thin low-temperature AlN or GaN buffer layers greatly helps to achieve good two-dimensional growth with a reduced density of misfit dislocations and other structural defects. Optimized GaN layers grown by MOCVD now have threading dislocation densities below 10^9 cm^{-2} (still extremely high

* Corresponding author. Tel: 00 49 89 2891 2760; Fax: 00 49 89 2891 2737; e-mail: stutz@wsi.tu-muenchen.de

PII S0925-9635(97)00204-5

compared with other group III–V or group II–VI epitaxial films, but apparently with no deleterious effects on devices) [5], with a rms surface roughness of 0.2 nm limited by step flow growth. In contrast, MBE grown GaN exhibits significantly rougher surfaces (about 1–2 nm rms), which moreover show little improvement upon implementation of a buffer layer. As an example, Fig. 1 shows a TEM micrograph of GaN directly grown on sapphire. The high density of dislocations and other defects at the interface decreases gradually within typically 1 μm as film growth proceeds. However, a high density ($\sim 5 \times 10^9$ cm^{-2}) of threading dislocation propagating parallel to the (0001) growth direction remains, even for thicker films. This can be compared with the CVD growth of highly oriented diamond on Si (100), where, starting from a highly defective nucleation layer, the crystallite size increases gradually with film thickness, until the entire growth surface is covered by {100} facets [6,7].

As mentioned above, a major advantage of AlGaN compared with diamond is the possibility to grow heterostructures for optical or charge carrier confinement. A problem could be the significant mismatch of approx. 3% between the lattice constants a_0 of GaN (0.3189 nm) and AlN (0.3112 nm) parallel to the substrate plane. Especially for large differences in the Al content and/or for thick overlayers the mismatch could give rise to structural relaxation with the generation of additional misfit dislocations. Fortunately, it turns out that the AlGaN alloys are rather well suited for pseudomorphic growth. This is demonstrated by Fig. 2, where we show high resolution X-ray diffraction results (reciprocal space map in the vicinity of the (002) reflex) obtained for a vertical laser structure consisting of a 150-nm thick GaN active layer embedded between two AlGaN Bragg-reflectors. Each reflector is built up by 20 bilayers (33 nm $Al_{0.2}Ga_{0.8}N$/38 nm $Al_{0.62}Ga_{0.38}N$). The total structure was deposited by MBE with a rf-plasma source and, according to Fig. 2, exhibits no signs of deviation from pseudomorphic growth.

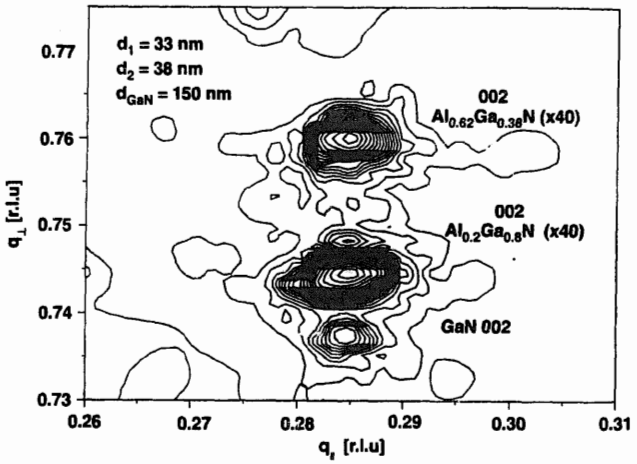

Fig. 2. Reciprocal space map in the vicinity of the 002 Bragg reflex of an AlGaN multilayer structure (GaN layer embedded between two Bragg reflectors of 20 pairs each). See text for further details.

3. Optical properties

AlGaN alloys are particularly attractive for optical applications in the ultraviolet spectral region, since the fundamental gap of AlGaN at 300 K can be adjusted

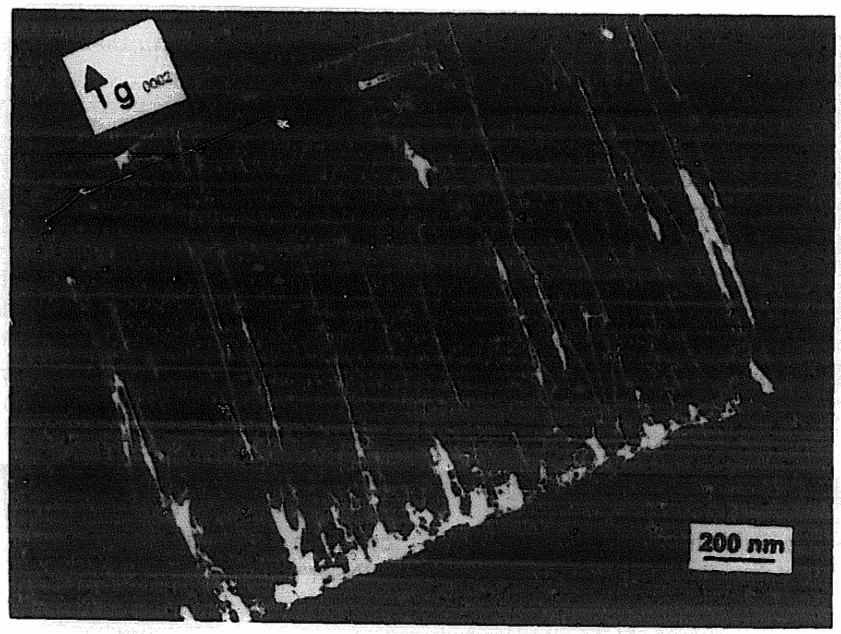

Fig. 1. Transmission electron micrograph of a GaN film grown by MBE on sapphire without the use of a buffer layer. Note the high density of misfit dislocations and other structural defects at the substrate interface. A high density of threading dislocations also persists further away from the substrate.

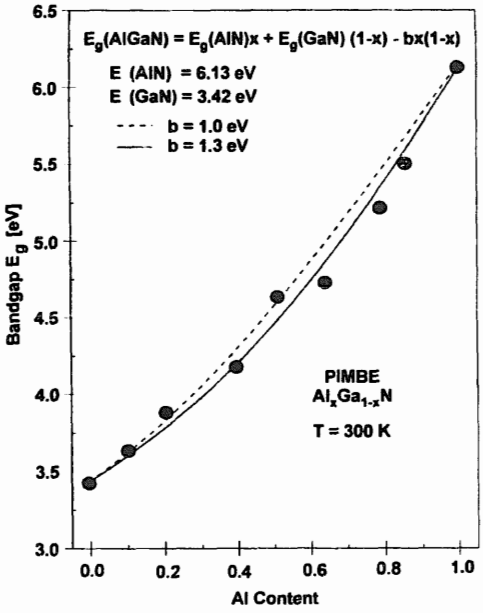

Fig. 3. Variation of the optical bandgap in AlGaN alloys with Al content.

continuously from 3.42 eV (GaN) to 6.13 eV (AlN). The dependence of the optical gap on Al content, x, is summarized in Fig. 3. The variation with x exhibits a slight deviation from linearity, characterized by a bending parameter of $b \sim 1.3$ eV. The nature of the optical gap remains direct, resulting in a sharp rise from a defect background with a linear absorption coefficient of approx. 300 cm^{-1} to the excitonic absorption edge with a coefficient of approx. 10^5 cm^{-1}. Accordingly, the optical transmission shows an almost step-like behavior at the band edge (Fig. 4). Moreover, the existence of

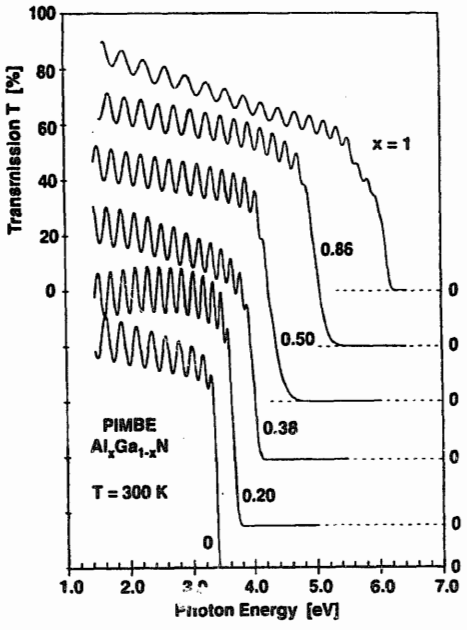

Fig. 4. Optical transmission spectra of AlGaN films on sapphire with different Al fraction.

pronounced interference fringes indicates the reasonable optical flatness of the epitaxial films. A more detailed discussion of the optical properties of MBE-grown AlGaN will be given in a forthcoming publication [8]. Here we only note that these basic optical properties of AlGaN are necessary conditions for the realization of filters, optical cavities, and interference structures e.g. for the use in light-emitters or selective UV detectors [9]. As an example of our own work, we show in Fig. 5 the reflectance spectra of the vertical laser structure already described above (c.f. Fig. 2).The strong (>94%) Bragg reflection around 370 nm together with the GaN cavity mode at 368 nm can be clearly seen. It is fairly safe to predict that because of the tunable optical properties of AlGaN this material system will play an important role in future UV electronic applications.

4. Electrical properties and doping

Nominally undoped GaN is usually n-type with an electron background concentration of 5×10^{16} cm^{-3}, probably coming from residual oxygen contamination. Deliberate n-type doping is possible e.g. with Si, (activation energy ≈ 20 meV) up to concentrations exceeding 10^{19} cm^{-3}. The electron effective mass is 0.22 m_0, the electron mobility at 300 K reaches values up to 1000 cm^2/Vs, depending on the structural quality of the material. p-type behavior can be achieved by doping with Mg. In MOCVD material, an additional annealing step at 700 °C is necessary to activate the Mg acceptors, most likely because of the formation of electrically inactive Mg–H complexes during cool-down in a hydrogen-containing atmosphere. MBE-grown Mg-doped samples do not require such an annealing step. Mg as the most common acceptor used today still has a rather large ionization energy of approx. 170 meV, so that less than 1% of the totally incorporated Mg acceptors are thermally activated at room temperature. Moreover, because of the large effective mass of holes

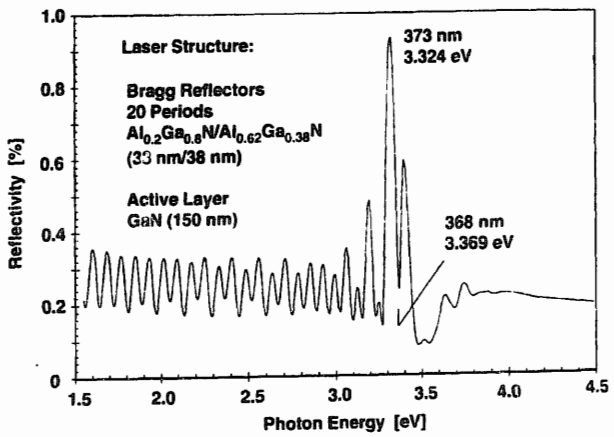

Fig. 5. Reflectance spectra of the vertical laser structure from Fig. 2.

in wurtzite GaN (approx. 1–2 m_0), the mobilities in typical p-type samples are less than 100 cm^2Vs^{-1}. Ohmic contacts to GaN can be achieved by Ti/Al or Ti/Au layers via the formation of an intermediate TiN phase. Good Schottky-contacts are more difficult to realize, requiring a careful cleaning of the GaN surface e.g. with a Ga beam in UHV. For a more detailed description of electronic transport and contact issues in GaN the reader is referred to Refs [2,3] and the references cited therein.

Thus, except for the low hole mobility, the electrical and doping properties of GaN appear much more favorable than those of CVD diamond, where efficient n-type doping is still elusive [10] and p-doping with boron also requires high concentrations, with the ensuing negative effects on carrier mobilities. In Fig. 6, we show a comparison between the subgap absorption spectra of undoped and boron doped CVD diamond and GaN grown by MBE. The spectra were obtained by the constant photocurrent method (CPM, see Ref. [11] for more details). In the diamond samples, the acceptor level at $E_V + 0.38$ eV is clearly seen by the onset of optical absorption from the valence band into the acceptor ground state, followed by the known phonon replica ([11] and references therein). Also visible is the enhanced absorption due to deep defects, which have a significantly lower contribution in undoped diamond. Qualitatively similar features are also observed in the GaN samples. Unfortunately, the expected onset of absorption at approx. 170 meV falls outside the accessible spectral range of our CPM setup, but the strongly enhanced infrared absorption and the contribution due to additional deep defects are clearly observed.

An important question in our comparison between CVD diamond and widegap AlGaN alloys, of course, is how these favorable properties of GaN change with increasing Al concentrations. We have therefore performed a systematic doping study over the entire compositional range. For n-type doping with Si (5×10^{19} cm^{-3}), the results are summarized in Fig. 7. Also included in this figure are measurements by Korakakis et al. for lower Al contents [12]. As a general trend, the Si donor ionization energy increases linearly with Al content from 20 meV in GaN to 320 meV in AlN, accompanied by an exponential decrease of the room temperature conductivity. A quantitative analysis of Hall experiments performed on Si-doped AlN at a higher temperature of 500 K gave an electron concentration of 10^{16} cm^{-3} and a Hall mobility of 5 cm^2 Vs^{-1}. In any case, unlike diamond and despite its large bandgap of more than 6 eV, MBE-grown AlN can still be doped n-type quite effectively.

In the case of p-type doping, a less encouraging picture emerges. Already small Al contents up to 30% lead to an increase of the conductivity activation energy from 170 meV in GaN to 360 meV in $Al_{0.27}Ga_{0.73}N$ (for a Mg concentration of 5×10^{19} cm^{-3}), showing that the acceptor ionization energy increases quickly with Al fraction (Fig. 8). This suggests that p-doping in AlGaN alloys with bandgaps above 5 eV will be much more difficult than p-doping of diamond. This is at least true for the case of Mg. Other dopants still need to be looked at in a systematic way. A second point of major concern is the influence of oxygen contamination, which becomes more important for increasing Al contents.

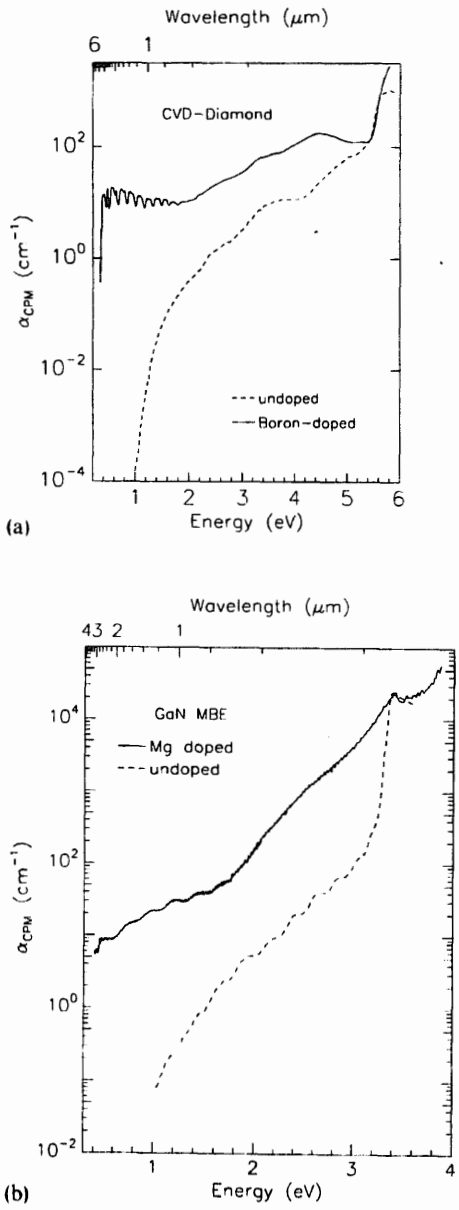

Fig. 6. Subgap absorption spectra of (a) undoped and boron-doped CVD diamond; and (b) undoped and Mg-doped GaN measured by the constant photocurrent method.

5. AlGaN-based devices

We finally discuss the potential use of AlGaN in electronic devices. Apart from preliminary investigations

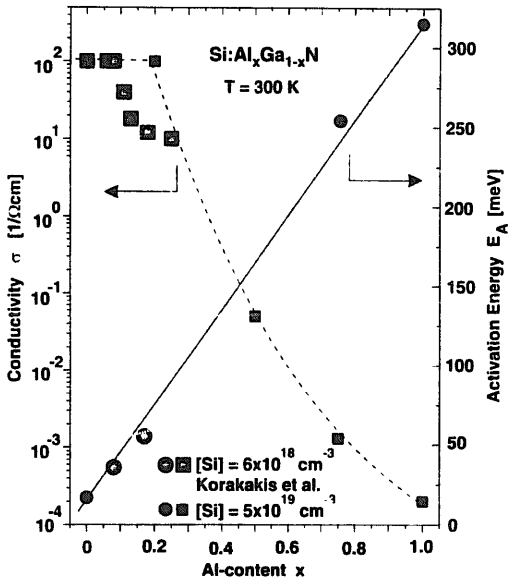

Fig. 7. Variation of the room temperature conductivity and the conductivity activation energy of Si-doped AlGaN with Al concentration. Data by Korakakis et al. for alloys with low Al content have also been included.

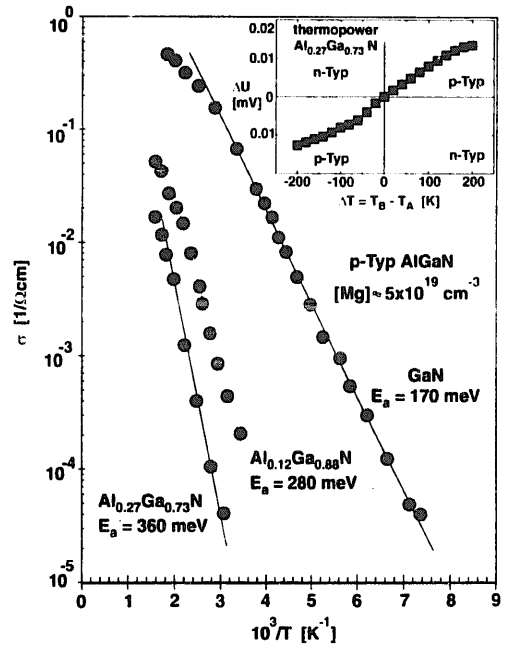

Fig. 8. Arrhenius plots of the dark conductivity of Mg-doped p-type GaN and two AlGaN alloys. Thermopower results (inset) show that the sample with the highest Al content is indeed p-type (Hall effect measurements were no longer possible because of the high resistivity).

of AlGaN p/n diodes or photodetectors already mentioned above, up to now most efforts have concentrated on the application in GaN/AlGaN hetero- and modulation-doped field-effect transistors (HFET and MODFET), using AlGaN barriers with Al concentrations below 20% [13–15]. A typical transistor structure consists of a 1-μm thick intrinsic GaN layer grown on sapphire with a n-type GaN channel followed by a thin (30 nm) AlGaN barrier layer. Depending on the design, the AlGaN barrier can also consist of a highly Si doped layer separated from the channel by a thin, undoped AlGaN spacer layer. Ohmic contacts to the channel and a Schottky gate contact complete the device. Further details are given in Refs [2,13–15]. Because of the large conduction band offset between GaN and AlN (1.8 eV [2]), already small Al contents are sufficient to produce a channel barrier much larger than kT. However, because of the high drift velocities in GaN (approx. 2.5×10^7 cm s^{-1} at 200 kV/cm) hot electrons are a concern and suggest the use of larger Al contents. Nevertheless, recently realized FET prototypes have shown impressive performance data, such as:

- current gain cut-off frequencies, $f_t = 30$ GHz, and maximum oscillation frequencies, $f_{max} = 97$ GHz, for 0.15 μm gates
- transconductances of 120 mS mm^{-1} at 300 K and 70 mS mm^{-1} at 800 K
- channel mobilities of 1200 cm^2 Vs^{-1} at 300 K and a carrier sheet density of 6×10^{12} cm^{-2}
- output power densities of 1.5 W mm^{-1} at 4 GHz.

Further improvements will certainly follow soon. As an example, with SiC as substrate material output powers up to 10 W/mm at 10 GHz can be reasonably projected. These results are similar or even superior to recently reported data for a diamond power FET grown by homoepitaxy on a type Ib diamond substrate [16].

A quite different application of AlGaN is its use in surface acoustic wave (SAW) devices. The velocity of the Rayleigh wave of AlN on sapphire with a (0001) surface (approx. 6000 m s^{-1}) is smaller than that of diamond, but on the other hand AlN is piezoelectric and provides a good electromechanical coupling without the use of hybrid transducers. As an example we show in Fig. 9 the first results obtained for epitaxial $Al_{0.75}Ga_{0.25}N$ films on sapphire grown by MBE which were used to produce delay lines of different lengths.

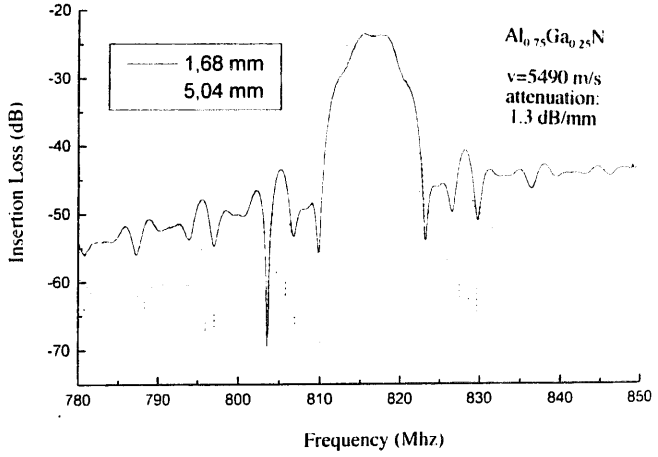

Fig. 9. Frequency characteristics of two AlGaN SAW-delay lines with different electrode distances.

These prototype devices exhibit an insertion loss of 25 dB and a linear attenuation of approx. 1.3 dB mm^{-1}. Using submicron contacts, operating frequencies in the GHz-range and, in particular, operating temperatures up to 1000 K should be achievable.

As a final point, we would like to mention that, similar to hydrogen-terminated diamond, AlN and AlGaN alloys with a large Al content exhibit the characteristics of a negative electron affinity (NEA) [17]. However, a systematic study under well-controlled surface conditions is still necessary for a better understanding of this feature. Interesting results are expected especially for AlGaN with different bulk Fermi level positions, which should give rise to different built-in fields at the surface. In this context the possibility to continuously vary the AlGaN bandgap and to dope AlGaN both n- and p-type should provide new opportunities for custom-made cold electron emitters.

6. Summary and conclusions

In this paper, we have given a brief overview over structural, electrical, and optical properties of AlGaN alloys. Compared with SiC or diamond, the AlGaN system has a number of interesting features, both from a basic physics point of view and for potential applications. A major advantage of AlGaN is the tunability of the fundamental bandgap over a wide energy range. This allows the design of novel optical devices in the UV spectral range and provides the basis for GaN/AlGaN heterostructure field-effect transistors, which hold much promise for high frequency, high power, and high temperature operation. Although the intrinsic electronic properties of AlGaN *a priori* should be inferior to those of diamond, the possibility to dope AlGaN over a wide compositional range both n- and p-type is an additional plus for this material system. It can be reasonably expected that further progress will occur in the near future, mainly linked to a better control of the heteroepitaxial growth of AlGaN on substrates such as sapphire and SiC.

Acknowledgement

Experimental support by and helpful discussions with S. Christiansen, M. Albrecht, Th. Kampen, W. Mönch, P. Gluche, E. Kohn, D. Brunner, C. Deger, R. Dimitrov and F. Freudenberg are gratefully acknowledged. This work was supported by the Deutsche Forschungsgemeinschaft and the Bayerische Forschungsstiftung.

References

[1] Physica Status Solidi (b) Vol. 202 (1997), and (a) Vol. 162 (1997): Special issue on Fundamental Questions and Applications of SiC, W.J. Choyke, H. Matsunami, G. Pensl (Eds)..
[2] S.N. Mohammad, A.A. Salvador, H. Morkoc, Proc. IEEE 83 (1995) 1306.
[3] GaN and Related Materials for Device Applications, in: S.J. Pearton, C. Kuo (Eds.), Mat. Res. Bull., February 1997.
[4] F.A. Ponce, D.P. Bour, Nature 386 (1997) 351.
[5] S.D. Lester, F.A. Ponce, M.G. Craford, D.A. Steigerwald, Appl. Phys. Lett. 66 (1995) 1249.
[6] C. Wild, R. Kohl, N. Herres, W. Müller-Sebert, P. Koidl, Diamond Relat. Mater. 3 (1994) 373.
[7] Y. von Kaenel, J. Stiegler, E. Blank, O. Chauvet, Ch. Hellwig, K. Plamann, Phys. Stat. Sol. (A) 154 (1996) 219.
[8] D. Brunner, H. Angerer, E. Bustarret, F. Freudenberg, R. Höpler, R. Dimitrov, O. Ambacher, M. Stutzmann, J. Appl. Phys. 82 (1997) 5090.
[9] D. Walker, X. Zhang, P. Kung, A. Saxler, S. Javadpour, J. Xu, M. Razeghi, Appl. Phys. Lett. 68 (1996) 2100.
[10] S. Koizumi et al., Appl. Phys. Lett. 71 (1997) 1065.
[11] E. Rohrer et al., these proceedings.
[12] D. Korakakis, H.M. Ng, K.F. Ludwig, T.D. Moustakas, Mat. Res. Soc. Symp. Proc. Vol. 449 (1996) 233.
[13] J. Burm, W.J. Schaff, L. Eastman, H. Amano, I. Akasaki, Appl. Phys. Lett. 68 (1996) 2849.
[14] Y.F. Wu, B.P. Keller, S. Keller, D. Kapolnek, P. Kozodoy, S.P. Denbaars, U.K. Mishra, Appl. Phys. Lett. 69 (1996) 1438.
[15] O. Aktas, Z.F. Fan, A. Botchkarev, S.N. Mohammad, M. Roth, T. Jenkins, L. Kehias, H. Morkoc, IEEE Electron. Device Lett. 18 (1997) 293.
[16] P. Gluche, A. Aleksov, A. Vescan, W. Ebert, E. Kohn, Proc. 55th Ann. Dev. Res. Conf., Fort Collins, USA, 1997.
[17] R.J. Nemanich, M.C. Benjamin, S.P. Bozeman, M.D. Bremser, S.W. King, B.L. Ward, R.F. Davis, B. Chen, Z. Zhang, J. Bernholc, Mat. Res. Soc. Symp. Proc. 395 (1996) 777.